Development of an impedimetric sensor based on carbon dots and chitosan nanocomposite modified electrode for Cu (II) detection in Water

mosaab echabaane (mosaab.echabaane@gmail.com)
Centre for Research on Microelectronics and Nanotechnology CRMN of Technopark of Sousse B.P.334
https://orcid.org/0000-0001-9230-3815

Salwa Hfaiedh
Centre for Research on Microelectronics and Nanotechnology CRMN of Technopark of Sousse B.P.334

Badreddine Smiri
Université de Monastir

Fawzi Saidi
Université de Monastir

Cherif Dridi
Centre for Research on Microelectronics and Nanotechnology CRMN of Technopark of Sousse B.P.334

Original Research Full Papers

Keywords: Carbon Dots, Chitosan, Nanocomposite, Copper(II), Impedimetric sensors

Posted Date: February 8th, 2021

DOI: https://doi.org/10.21203/rs.3.rs-191753/v1

Abstract

The fast and sensitive detection of copper ions would be essential for water monitoring. Herein, we report a novel development of impedimetric sensor based on carbon dots/chitosan nanocomposite. Carbon dots (CDs) were synthesized by simple heating of acidic aqueous solution of glucose. The CDs were characterized by TEM, FTIR, XRD, UV-visible, and PL. These measurements revealed that the CDs possess a mean size of 3.2 nm, graphitic structure with carboxyl and hydroxyl groups on the surface, and show particular optical properties. A glassy carbon electrode (GCE) was modified with a carbon dots/chitosan (CHITO) nanocomposite, and was characterized by transmission electron microscopy and electrochemical impedance spectroscopy (EIS). The CDs-CHITO/GCE electrode exhibits large surface area, good conductivity film, and charge transfer at interface film/electrolyte. The proposed impedimetric sensor exhibits a linear response to Cu(II) over 10^{-9} M to 10^{-5} M rang with a limit of detection at about 5×10^{-10} M. In addition, the sensor shows good selectivity toward Cu(II) ions, which is less than 5 %.

Therefore, the as-developed impedimetric sensor exhibits good reproducibility, stability, selectivity, and a low limit of detection, which augur well for its application in water safety control processes.

1. Introduction

Nowadays, the determination of heavy metals ions is highly significant for human health and environmental safety. One of the heavy metal ions, copper is the third most abundant metal ion that plays vital roles in various biological functions in human beings such as blood formation, connective tissue development, transcriptional events and the functioning of several enzymes [1]. However, Excess of copper ions can cause gastrointestinal disturbance, neurodegenerative diseases, and kidney and liver damage [2]. The World Health Organization (WHO) decided the permissible limit of Cu^{2+} ions in drinking water at 30 nM [3, 4]. Thus, it is important to determine the low concentration of copper in the environmental.

Several methods for the determination of copper ions have been proposed such as atomic absorption spectroscopy, chromatography spectrofluorimetry, and spectrophotometry [5–8]. However, these methods are high cost, time-consuming, not easy to control. Therefore, to avoid these drawbacks, the electrochemical sensor has attracted great attention, for the detection of copper ion, because of their intrinsic advantages such as simple operation, high sensitivity, low cost, rapidity, high sensitivity and selectivity [9].

Notably, the modification of the electrode surface with advanced nanomaterials has significantly enhanced the sensitivity and selectivity of the sensor [10–12]. Among nanostructured materials, nanocomposites have attracted potential in the development of electrochemical sensors. [13–14]. The nanocomposites prepared by combination or functionalization of two organic and inorganic nanomaterials, which exhibit, good catalytic activity, high large surface areas, better thermal stability, provide good conductivity and improve the selectivity of sensing metal ions [15–16]. Recently, the

nanocomposite a based Chitosan and carbonaceous nanoparticles have much interest for the design and elaboration of the electrochemical sensors [17–20].

Chitosan exhibits interesting properties such as nontoxicity, film-forming ability, high permeability, adsorption ability, and biocompatibility. It has been considered as a favorable biomaterial for constructions of sensors [21].

One of the most important nanostructured carbon, CDs have received major attention and appear as new alternatives due to their properties excellent physical, chemical, high conductivity, environmental friendliness, high biocompatibility, high surface area, simple synthetic routes and surface functionalization [22–24]. In this context, the nanocomposite can be prepared by dispersion CDs in CHITO to enhance the electrochemical properties for chemical sensing applications.

In this work, we have developed impedimetric sensors based on a carbon dots (CDs) and chitosan (CHITO) nanocomposite modified glassy carbon electrode (CDs-CHITO/GCE) for the detection of copper. The carbon dots were synthesized from glucose by simple heating, and were characterized by the transmission electron microscope (TEM), X-ray diffraction (XRD), FTIR spectroscopy, UV-vis absorption and photoluminescence spectroscopy. The nanocomposite was deposited onto the GCE electrode by drop-casting. The morphological and electrochemical properties of nanocomposite were investigated by scanning electronic microscopy (SEM), and electrochemical impedance spectroscopy (EIS). The linear range, limit detection, reproducibility and selectivity of the prepared sensors was discussed. The CDs-CHITO/GCE sensor was applied to determine cooper ions in real water samples.

2. Experimental

2.1. Materials

Sulfate copper ($CuSO_4$), mercury nitrate ($Hg(NO_3)_2$), cadmium nitrate ($Cd(NO_3)_2$), lead nitrate ($Pb(NO_3)_2$), Nickel nitrate ($Ni(NO_3)_2$), zinc nitrate ($Zn(NO_3)_2$), Sodium chloride (NaCl), chlorure calcium $CaCl_2$) potassium chloride (KCl), glucose powder, sulphuric acid (H_2SO_4), DI water, sodium hydroxide (NaOH), ammonium acetate (CH_3COO^-, NH_4^+), and chitosan (CHITO). All chemicals used in this work were purchased from of Sigma- Aldrich.

2.2. Synthesis of carbon dots (CDs) from Glucose

3 g of glucose powder and 1 ml of H□SO□ were dissolved in 10 ml of DI water. Then, the solution was stirred at a temperature of 100° C (Fig. 1). A yellow-brownish color was obtained indicating the formation of CDs. The NaOH was neutralized the solution. The mixture was centrifuged at 14000 rpm, was filtered, and dried at a temperature of 80°C for 6 hours.

2.3. Preparation of modified Glassy Carbon Electrode (GCE)

The surface of the bare GCE electrode was polished with powder of alumina of 0.05 µm and 0.3 µm. Then, the electrode washed with distilled water, ethanol, and distilled water successively in an ultrasonic bath, and dried at room temperature before use.

In the development of the chemical sensor, we have used the chitosan to facilitate the immobilization of carbon dots on GCE electrode and improve sensing of surface property. The CHITO-CDs nanocomposite solutions were prepared by prepared by the following procedure. 0.5 mL of 1.0% CHIT solution was added to 1.5 mL of CDs solution with ultrasonication.

Then, 8 µL of the mixture solution was dropped on the surface of the electrode and it was dried at 60°C for 30 min.

2.4. Instrumentation

The synthesized CDs were selected for further study via Transmission Electron Microscope (TEM) (JEOL JEM 2010), X-ray diffractometer (Bruker AXS D8 Advance), Fourier Transform Infrared Spectroscopy (FTIR) (Perkin Elmer, Spectrum Two), UV–vis spectrophotometry (Specord 210 Plus), and spectrophotometer (HORIBA Jobin Yvon). The CHIT-CDs nanocomposite film were characterized by Scanning Electron Microscopy (SEM) (Jeol JSM-5400 emission) and impedance analyzer (EC-LAB BIOLOGIC). The electrochemical impedance spectroscopy (EIS) measurements were carried in the 0.01 Hz-100 kHz frequency ranges with sinusoidal excitation signal amplitude of 10 mV. The electrochemical cell formed by two components: an electrolyte (ammonium acetate, 0.1 M, pH = 7) and three electrodes (working electrode (GCE), counter electrode (platinum), reference electrode (Ag/AgCl)).

3. Results And Discussion

3.1. Characterization of Carbon dots

To further explore the morphology, structure, chemical functionalities, and optical of CDs, we used the transmission electron microscope (TEM), X-ray diffraction (XRD), FTIR, UV-Vis absorption, and photoluminescence spectroscopies.

The TEM image of the prepared CDs is shown in Fig. 2a. It is observed that the CDs are spherical in shape; narrow size distribution and the size are distributed in the range of 1.5-6 nm (3.2 nm mean size of CDs).

The X-ray diffraction (XRD) pattern of CDs is exhibited in Fig. 2b. The spectrum showed a broad peak at 2θ= 22.35°, corresponding to (002) hkl plane of the graphitic structure [25,26].

Fig. 1c shows the FTIR transmittance spectrum of the CDs. The peaks at 3319 cm^{-1}, 1727 cm^{-1}, 1642 cm^{-1} and 1092 assigned to O-H, C = O, C = C and C-O, respectively [27-28]. The results reveal that carboxyl and hydroxyl groups exist on the surface of CDs.

As shown in Fig. 2d, The UV-Vis absorption spectrum of CDs exhibited two absorption band located at 280 nm and 375 nm , which are ascribed to π-π* and n-π* which are ascribed to the π-π* and n-π* transitions of C=C and C=O bonds, respectively. From this spectrum, band gap energies of CDs were calculated using Eq.1[29]

$$E_g = \frac{1240}{\lambda_{edge}} \quad (1)$$

,where **λedge** is the onset value of the absorption bands most intense. The optical band gap (Eg) was estimated to be 3.52 eV.

Fig. 2e presents the PL spectrum of the CDs excited at 360 nm. It noted that the PL emission peak of CDs located at 470 nm is the blue light luminescent spectral region [30]. Additionally, the PL spectrum shows a wide PL band with the full width at half maximum (FWHM) of 135 nm, this is related to the effect distribution of the different size of the CDs. To inform the origin of luminescent of CDs, The PL spectrum is fitted by two Gaussian bands (Fig. 2e). The first band (E_{m1}) at 440 nm is attributed to radiative recombination of clusters of carbon dots and the second band (E_{m2}) at 515 nm is assigned to the surface states of CDs [31].

3.2. Characterization of the functionalized GCE

Surface morphology of the bare GCE electrodes and functionalized witch CHITO and CHITO-CDs nanocomposite film are investigated by SEM. The bare GCE electrode displays a flat and smooth surface (Fig. 3a). Further, the CHITO surface layer is rough and uniformly distributed on GCE electrode the surface (Fig. 3b). After the addition of CDs into CHITO (Fig. 3c), the surface of CHITO-CDs nanocomposite film is rough and few apparent pores. Thus, the addition of CDs provided a large active surface area for CHITO-CDs /GCE electrode.

For sensor measurements, the potential polarization has a vast influence on impedimetric sensor response since it leads to an improved sensitivity for the recognition of the target analyte [32]. Fig. 4 shows the impedance spectra of the CHIT/CGE electrode at different potentials: 0, 0.2, 0.4, and 0.6 V vs. Ag/AgCl. Under bias voltages, the Warburg straight line and the impedance spectra decreased. It noticed that the best diameter of the half-circle was found at 0.6 V vs. Ag/AgCl, which can be allowed to observe the ions kinetic at the film/electrolyte interface [33]. Hence, the potential polarization is selected at 0.6 V along with the following work.

Nyquist diagrams of the bare GCE electrodes and functionalized witch CHITO and CHITO-CDs nanocomposite film are presented in Fig. 5. It is noted that the diameters of the semi-circle increase after the functionalization film on the GCE electrode. This is attributed to the immobilization of the membrane. However, it is observed that the decrease of Nyquist for CHITO-CDs/GCE structure compared to CHITO/CGE structure. This is due to the variation of the electric properties of the film with the incorporation of CDs.

The impedance spectra of functionalized GCE electrodes were fitted using the equivalent circuits illustrated in Fig. 6. This circuit model is a combination of three parts. The first component is a series resistance of the electrolyte solution (R_s). The second component at higher frequencies, which is attributed to the electrode/ film interface, is formed by a film resistance (R_f) and a film capacitance (CPE_f). The last component the last component at the low frequency, which is described to the film/electrolyte interface, is consisted of a charge transfer resistance (R_{itc}) and a double layer capacitance (CPE_{dl}). The values reached from the fitting model using “Zview “software are given in Table 1, escorted with the total error (χ^2).

To provide information on the electrical properties of the CHITO-CDs/GCE and CHITO/CGE structures, the values of R_f and R_{itc} are studied. As it has been seen in the Table 1, the R_f value of the CHIT film has been 35.98 kΩ. While the CHITO-CDs film, the R_f value has been decreased to 22.58 kΩ, indicating that CDs improves the electrical conductivity.

Moreover, the R_{itc} parameter of the CHIT modified electrode has been 99.50 kΩ. For the CHITO-CDs modified electrode, the R_{itc} value has been decreased to 83.42 kΩ, indicating the enhancement charge transfer.

Hence, additional CDs improves the conductivity of the film, increases the surface area and facilitates charge transfer at the film/electrolyte interface. This clearly proves that the CHITO-CDs/GCE structures can be used as promising candidate for impedimetric sensor application.

3.3. Detection of Copper ion

The electrochemical response of copper at the CHITO/GCE and CHITO-CDs/GCE is examined using EIS in various concentrations of Cu^{2+} ions.

The Nyquist plot of the two structures after the addition of concentration of Cu^{2+} ion (from 10^{-9} to 10^{-5} M) are shown in Fig. 7a and 7b. It is mentioned that the total impedance decreased slightly for CHIT modified electrode with the increase of copper concentrations, whereas, the diameter of the impedance spectra of the CHITO-CDs modified electrode decreased clearly by the addition of the Cu^{2+} concentrations. This is indicates that the nanocomposite film has more sensitivity versus Cu(II) ions comparing to CHITO film. Thus, the adding CDs improved the sensing property to Cu^{2+}ions.

The response of CHITO-CDs modified electrode to Cu^{2+} ions is due to the complexation process (Fig. 8). This is induced by electrostatic interaction between the donor groups of nanocomposites and the copper ion, where the donor groups are CDs, hydroxyl, and amide.

Indeed, the addition of CDs increases surface area, gives more active sites, and facilitated the interaction between the CHIT-CDs modified electrode surface and copper ions.

It is for this reason that further experiments were carried using CHITO-CDs/GCE structure to detect copper ions.

The equivalent electrical circuit described above has been used to fit the experimental impedance data related to the copper detection. The values of electrical parameters are illustrated in Table 2.

It is observed from Table 2 that the value of R_f remains relatively constant by the addition of Cu^{2+} ion. This can be indicated that the copper ion interacts only on the CHITO-CDs modified electrode surface. However, the value of R_{it} decreases when increasing the concentration of copper ion, leading to the strong interactions between nanocomposites and Cu^{2+} ion and enhancement the charge transfer to the film/electrolyte interface. Therefore, the charge transfer resistance is presented as the main parameter influencing on the response of the sensors to copper ions.

Indeed, the calibration curve of the sensor for copper detection is determined by plotting the variation of R_{it} (Fig. 9). The Fig. 9 illustrates the variation of ΔR_{it} ($R_{it(}$electrolyte)-$R_{it(Copper)}$) as a function of log [Cu^{2+}], where $R_{it(}$electrolyte) is the charge transfer resistance before the addition of copper solution (blank test) and $R_{it(Copper)}$ is the charge transfer resistance value from sensors after adding of the different concentrations of copper.

This plot showed a linear region from 10^{-9} M to 10^{-5} M. The equation of linear regression is $\Delta R_{it}(K\Omega)$= 9.98 × (log[C/nM]) + 16.63) (R^2=0.9986), where the slope is 9.98 of the sensors sensitivity. The limit detection was estimated to be 5×10^{-10} M according to the formula LOD= (3 ×Standard deviation)/slope.

The analytical performance of CHITO-CDs/GCE structure based impedimetric copper sensors was compared with other chemical sensors from the literature, as seen in Table 3 and shows the as proposed impedimetric sensor with an easy and simple preparation process shows a broad linear range and the lowest limit of detection (LOD).

3.4. Reproducibility and Interference

The reproducibility of the impedimetric sensor at CHITO-CDs/GCE was examined by three measurements of the response to 10^{-6} M copper in the electrolyte (pH 7.0). The relative standard deviation (RSD) was found to be around 3.93%. This shows that the proposed sensors has good reproducibility.

The selectivity of the proposed impedimetric sensor towards Cu^{2+} ion was examined in the presence of interfering ions at concentrations 100-fold higher than that of Cu(II) ions. The interferents ions including Hg^{2+}, Cd^{2+}, Pb^{2+}, Ni^{2+}, Zn^{2+}, Na^{+}, Ca^{+} and K^{+} was tested.

Fig.10 presents relative signal change $\left(\left[\frac{R_{it}-R_{it0}}{R_{it0}}\right]\right)$ in the presence of these interferents. Where R_{it0} and R_{it} are the resistances of charge transfer corresponding to the sensor response towards Cu^{2+} ion in the

absence and presence *of the interfering ion,* respectively. It is noted from this figure that the relative signal change is less than 5%. The results indicated that CHITO-CDs/GCE structure exhibited good selectivity to Cu^{2+} in the presence of the other ions.

3.4. Determination of copper ion in water samples

To evaluate the practical feasibility of the CHITO-CDs/GCE impedimedric sensor is applied for the determination of Cu^{2+} ions in different water samples (tap and well water). One milliliter of each sample solution is added to 1 mL of electrolyte at pH 7. Then, the analysis is carried by the EIS method. The spiked Cu^{2+} amounts are of 10^{-6} M and 10^{-8} M. It can be seen in Table 4 that the recoveries in the range of 96.54% and 103.8%, which is less than 5 % . The results show that the proposed CHIT-CDs/GCE impedimetric sensor is efficient for the detection of copper ion in real water samples.

4. Conclusions

A facile and a low-cost electrochemical impedemetric sensor for copper ions detection has been developed with a sustainable approach based on carbon dots/chitosan nano-bio-composites electrochemical impedance spectroscopy has been shown to be a very sensitive tool for analytical copper ions detection. The as developed impedemetric sensor has show good selectivity and reproducibility with a high sensitivity and a very low limit of detection. The as prepared highly sensitive Cu sensor provides a promising cost-effective nano platform for water monitoring applications.

Declarations

Funding information

The authors received financial support from the Ministry of Higher Education and Scientific Research of Tunisia.

References

1. M.N. Majd, M.A. Taher, M. Fazelirad, Preparation and application of a simple electrochemical sensor for the determination of copper in some real and standard samples. Ionics **22**, 289-296 (2016)
2. R. Hu, H. Gou, Z. Mo, X. Wei, Y. Wang, Highly selective detection of trace Cu^{2+} based on polyethyleneimine-reduced graphene oxide nanocomposite modified glassy carbon electrode. Ionics **21**, 3125-3133 (2015)
3. T. Wu, T. Xu, Z. Ma, Sensitive electrochemical detection of copper ions based on the copper (II) ion assisted etching of Au@ Ag nanoparticles. Analyst **140**, 8041-8047 (2015)
4. L. Cui, J. Wu, J. Li, Y. Ge, H. Ju, Electrochemical detection of Cu^{2+} through Ag nanoparticle assembly regulated by copper-catalyzed oxidation of cysteamine. Biosens. Bioelectron. **55**, 272-277 (2014)

5. M. Soylak, I. Narin, M. Dogan, Trace enrichment and atomic absorption spectrometric determination of lead, copper, cadmium and nickel in drinking water samples by use of an activated carbon column. Anal. Lett. **30**, 2801-2810 (1997)
6. A. Ali, H. Shen, X. Yin, Simultaneous determination of trace amounts of nickel, copper and mercury by liquid chromatography coupled with flow-injection on-line derivatization and preconcentration. Anal. Chim. Acta. **369**, 215-223 (1998)
7. M. Amjadi, Z.A. Fakhri, Gold nanostar-enhanced chemiluminescence probe for highly sensitive detection of Cu (II) ions. Sensors Actuators B Chem. **257**, 629-634 (2018)
8. N.K. Agnihotri, V.K. Singh, H.B. Singh, Derivative spectrophotometric determination of copper (II) in non-ionic micellar medium. Talanta **45**, 331-341(1997)
9. I. Kaur, M. Sharma, S. Kaur, A. Kaur, Ultra-sensitive electrochemical sensors based on self-assembled chelating dithiol on gold electrode for trace level detection of copper (II) ions. Sensors Actuators B Chem. **312**, 127935-127946 (2020)
10. Y. Wei, Z. Xu, S. Wang, S. Liu, D. Zhang, Y. Fang, One-step preparation of carbon quantum dots-reduced graphene oxide nanocomposite-modified glass carbon electrode for the simultaneous detection of ascorbic acid, dopamine, and uric acid. Ionics **26**, 5817-5828 (2020)
11. E. Muthusankar, S.W. Mohammad, Z.A. Alothman, M.R. Johan, V.K. Ponnusamy, D. Ragupathy, Fabrication of amperometric sensor for glucose detection based on phosphotungstic acid–assisted PDPA/ZnO nanohybrid composite. Ionics **26**, 6341-6349 (2020)
12. A. Mahmoud, M. Echabaane, K. Omri, L. ElMir, R.B. Chaabane, Development of an impedimetric non enzymatic sensor based on ZnO and Cu doped ZnO nanoparticles for the detection of glucose. J. *Alloys Compounds***786**, 960-968(2019)
13. S. Jebril, L.C. Aguilera, J.M.P. Santander, C. Dridi, A novel electrochemical sensor modified with green gold sononanoparticles and carbon black nanocomposite for bisphenol A detection. Mater. Sci. Eng. B **264**, 114951-114961 (2021)
14. G. Padmalaya, B. S. Sreeja, S. Shoba, R. Rajavel, S. Radha, M. Arivanandan, S, Shrestha, Synthesis of Micro-dumbbell Shaped rGO/ZnO Composite Rods and Its Application Towards as Electrochemical Sensor for the Simultaneous Determination of Ammonia and Formaldehyde Using Hexamine and Its Structural Analysis. J. Inorg. Organomet. Polym. Mater. **30**, 943-954 (2020)
15. D. F. Katowah, Q. A. Alsulami, M. M. Alam, S. H. Ismail, Abdullah M. Asiri, G. G. Mohamed, M. M. Rahman, M. A. Hussein, The Performance of Various SWCNT Loading into CuO-PMMA Nanocomposites Towards the Detection of Mn^{2+} Ions. J. Inorg. Organomet. Polym. Mater. **30**, 5024-5041 (2020)
16. S.L. Wei, L.J. Yan, J.W. Li, S. Yao, H.S. Zhang, A.Z. Xu, Facile and green fabrication of electrochemical sensor based on poly(glutamic acid) and carboxylated carbon nanosheets for the sensitive simultaneous detection of Cd(II) and Pb(II). Ionics **27**, 375-387 (2021)
17. M. Rizwan, S. Elma, S.A. Lim, M.U. Ahmed, AuNPs/CNOs/SWCNTs/chitosan-nanocomposite modified electrochemical sensor for the label-free detection of carcinoembryonic antigen. Biosens.

Bioelectron. **107**, 211-217 (2018)

18. J. Huang, Z. Xie, Y. Huang, L. Xie, S. Luo, Q. Fan , T. Zeng, Y. Zhang, S. Wang, M. Zhang, Z. Xie, X. Deng, Electrochemical immunosensor with Cu (I)/Cu (II)-chitosan-graphene nanocomposite-based signal amplification for the detection of newcastle disease virus. Sci. Rep. **10**, 1-12 (2020)
19. C.S. Comino, I. Rassas, S. Minot, F. Bessueille , M. Arab , V. Chevallier, M.L.R. Mendez , A. Errachid, N.J. Renault, Voltammetric Sensor Based on Molecularly Imprinted Chitosan-Carbon Nanotubes Decorated with Gold Nanoparticles Nanocomposite Deposited on Boron-Doped Diamond Electrodes for Catechol Detection. Materials **13**, 688-699 (2020)
20. F. Jalali, Z. Hassanvand, A. Barati, Electrochemical Sensor Based on a Nanocomposite of Carbon Dots, Hexadecyltrimethylammonium Bromide and Chitosan for Mesalazine Determination. J. Anal. Chem. **75**, 544-552 (2020)
21. F. Nazari, S.M. Ghoreishi, A. Khoobi, Bio-based Fe3O4/chitosan nanocomposite sensor for response surface methodology and sensitive determination of gallic acid. INT. J. BIOL. MACROMOL. **160**, 456-469 (2020)
22. S.Y. Lim, W. Shen, Z. Gao, Carbon quantum dots and their applications. Chem. Soc. Rev. **44**, 362-381 (2015)
23. X. Wang, Y. Feng, P. Dong, J. Huang, A Mini Review on Carbon Quantum Dots: Preparation, Properties and Electrocatalytic Application. Front. Chem. **7**, 671-680 (2019)
24. S. Campuzano, P.Y. Sedeño, J.M. Pingarrón, Carbon dots and graphene quantum dots in electrochemical biosensing. Nanomaterials **9**, 634-652 (2019)
25. X. Teng, C. Ma, C. Ge, M. Yan, J. Yang, Z. Ye, P.C. Moraiscd, H. Bi, Green synthesis of nitrogen-doped carbon dots from konjac flour with “off–on” fluorescence by Fe^{3+} and L-lysine for bioimaging. J. Mater. Chem. B **2**, 4631-4639 (2014)
26. N. Vasimalai, V.V. Boas, J. Gallo, M.F. Cerqueira, M.M. Miranda, J.M.C. Fernández, L. Diéguez, B. Espiña, M.T.F. Argüelles, Green synthesis of fluorescent carbon dots from spices for in vitro imaging and tumour cell growth inhibition. Beilstein J. Nanotechnol. **9**, 530-544 (2018)
27. J.P. Naik, P. Sutradhar, M. Saha, Molecular scale rapid synthesis of graphene quantum dots (GQDs). J. Nanostructure Chem. **7**, 85-89 (2017)
28. Z. Chen, J. Wang, H. Miao, L. Wang, S. Wu, X. Yang, Fluorescent carbon dots derived from lactose for assaying folic acid. Sci. China. Chem. **59**, 487-492 (2016)
29. F. Yuan, Z. Wang, X. Li, Y. Li, Z. Tan, L. Fan, S. Yang, Bright multicolor bandgap fluorescent carbon quantum dots for electroluminescent light-Emitting diodes. Adv. Mater. **29**, 1604436-1604442 (2017)
30. A.B. Siddique, V.P. Singh, S. Chatterjee, A.K. Pramanik, M. Ray, Facile synthesis and versatile applications of amorphous carbon dot. Materials Today **5**, 10077-10083 (2018)
31. snaeni, Y. Herbani, M.M. Suliyanti, Concentration effect on optical properties of carbon dots at room temperature. J. Lumin. **198**, 215-219 (2018)

32. D. Najlaoui, M. Echabaane, A.B. Khélifa, A. Rouis, H.B. Ouada, Photoelectrochemical impedance spectroscopy sensor for cloxacillin based on tetrabutylammonium octamolybdate. J. SOLID. STATE ELECTR. **23**, 3329-3341 (2019)
33. A. Rouis, M. Echabaane, N. Sakly, I.D. Bonnamour, H.B. Ouada, Electrochemical analysis of a PPV derivative thin film doped with ß-ketoimine calix[4]arene in the dark and under illumination for the detection of Hg^{2+} ions. Synth. Met. **164**, 78-87 (2016)
34. S. Wang, J. Li, Y Qiu, Y. Zhuang, X. Wu, J. Jiang, Facile synthesis of oxidized multi-walled carbon nanotubes functionalized with 5-sulfosalicylic acid/MoS_2 nanosheets nanocomposites for electrochemical detection of copper ions. Appl. Surf. Sci. **487**, 766-772 (2019)
35. X. Liu, J. Han, X. Hou, F. Altincicek, N. Oncel, D. Pierce, X. Wu, J.X. Zhao, One-pot synthesis of graphene quantum dots using humic acid and its application for copper (II) ion detection. J. Mater. Sci. **56**, 4991-5005 (2021)
36. 36. S.M. Saleh, R. Ali, M.E.F. Hegazy, F.M. Alminderej, T.A. Mohamed, The natural compound chrysosplenol-D is a novel, ultrasensitive optical sensor for detection of Cu(II). J. Mol. Liq. **302**, 112558-112565 (2020)
37. S.D. Masi, A. Pennetta, A. Guerreiro, F. Canfarotta, G.E.D. Benedetto, C. Malitesta, Sensor based on electrosynthesised imprinted polymeric film for rapid and trace detection of copper(II) ions. Sensors Actuators B Chem. **307**, 127648-127656 (2020)
38. J. Yu, X. Zhang, M. Zhao, Y. Ding, Z. Li, Y. Ma, H. Cui, Fabrication of the Ni-based composite wires for electrochemical detection of copper(□) ions. Anal. Chim. Acta **25**, 45-52 (2021)
39. W. Xiong, P. Zhang, S. Liu, Y. Lv, D. Zhang, Catalyst-free synthesis of phenolic-resin based carbon nanospheres for simultaneous electrochemical detection of Cu (II) and Hg (II). Diam. Relat. Mater. **111**, 108170-108178 (2021)

Tables

Table 1 Fitting parameters of Nyquist plots for bare GCE, CHITO/CGE, and CHITO-CDs/CGE Electrodes

electrodes	R_s (kΩ)	CPE_f (μF)	n_1	R_f (kΩ)	CPE_{dl} (μF)	n_2	R_{it}(kΩ)	$\chi^2(10^{-4})$
Bare CGE	0.14	-	-	-	5.2	0.90	51.40	9.3
CHIT/ CGE	0.15	1.30	0.88	35.98	5.14	0.63	99.50	3.7
CHIT-CDs / CGE	0.13	1.40	0.90	22.58	9.18	0.51	83.42	7.3

Table 2 Fitting parameters of CHITO-CDs/GCE versus copper concentrations

$[Cu^{2+}]$ (mol L^{-1})	R_s (kΩ)	CPE_f (μF)	n_1	R_f (kΩ)	CPE_{dl} (μF)	n_2	R_{it}(kΩ)	$\chi^2(10^{-4})$
10^{-9}	0.11	1.70	0.90	17.40	9.20	0.59	67.24	2.7
10^{-8}	0.10	1.73	0.89	16.24	10.01	0.60	56.56	6.8
10^{-7}	0.11	1.60	0.88	15.01	9.22	0.60	45.05	7.3
10^{-6}	0.12	1.56	0.90	13.40	9.52	0.61	36.16	2.1
10^{-5}	0.13	1.66	0.88	12.50	10.10	0.62	27.72	4.2

Table 3 Comparison of several materials for Cu (II) sensing

Electrode material	Analytical technique	Linear range (M)	Limit of Detection (M)	Reference
SSA/MoS_2/oMWCNTs	DPV	1×10^{-7}-11×10^{-6}	5.7×10^{-8}	[34]
GQDs	Fluorescence	1×10^{-6}-4×10^{-5}	4.4×10^{-7}	[35]
Chp-D	Fluorescence	4×10^{-8}-1. 10^{-6}	1.2×10^{-8}	[36]
IIP film	DPV	9×10^{-10}-1.5. 10^{-8}	2.7×10^{-9}	[37]
Ni/NiO/ZnO-6/CS	DPV	0 - 6×10^{-6}	8.1×10^{-10}	[38]
OP30-2.0-CSs	DPASV	0 - 5×10^{-6}	2×10^{-9}	[39]
CHITO-CDs	EIS	**10^{-9}- 10^{-5}**	**5×10^{-10}**	**This work**

SAA:5-sulfosalicylic acid; MoS_2: molybdenum disulfide nanosheets; oMWCNTs: oxidized multi-walled carbon nanotubes;GQDs: graphene quantum dots; Chp-D: Chrysosplenol-D; IIP: ion imprinted polymer; Ni: Nickel wire; NiO: Nickel Oxide; Zinc Oxide; CS: Chitosan; OP30-2.0: Octaphenyl polyoxyethyiene-30 (OP-30); CSs: carbon nanospheres.

Table 4 Determination of copper ion in tap and well

Samples	Added (M)	Found (M)	Recovery (%)
Tap water	10^{-8}	9.714×10^{-9}	97.14
	10^{-6}	1.023×10^{-6}	102.3
Well wate	10^{-8}	9.654×10^{-9}	96.54
	10^{-6}	1.038×10^{-6}	103.8

Figures

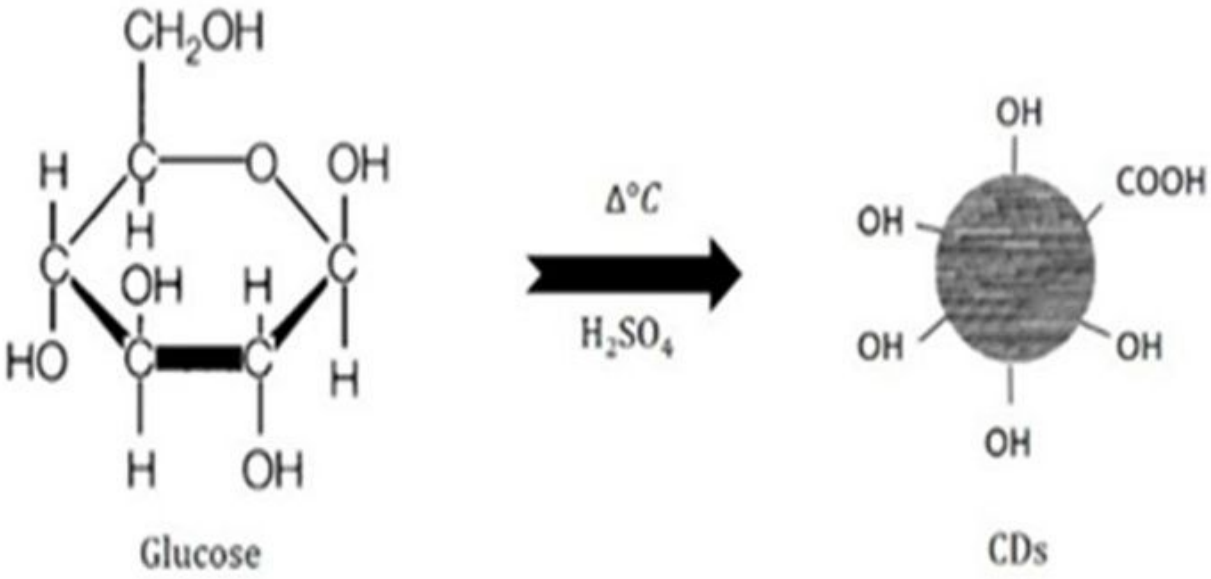

Figure 1

Schematic representation of CDs formation from glucose

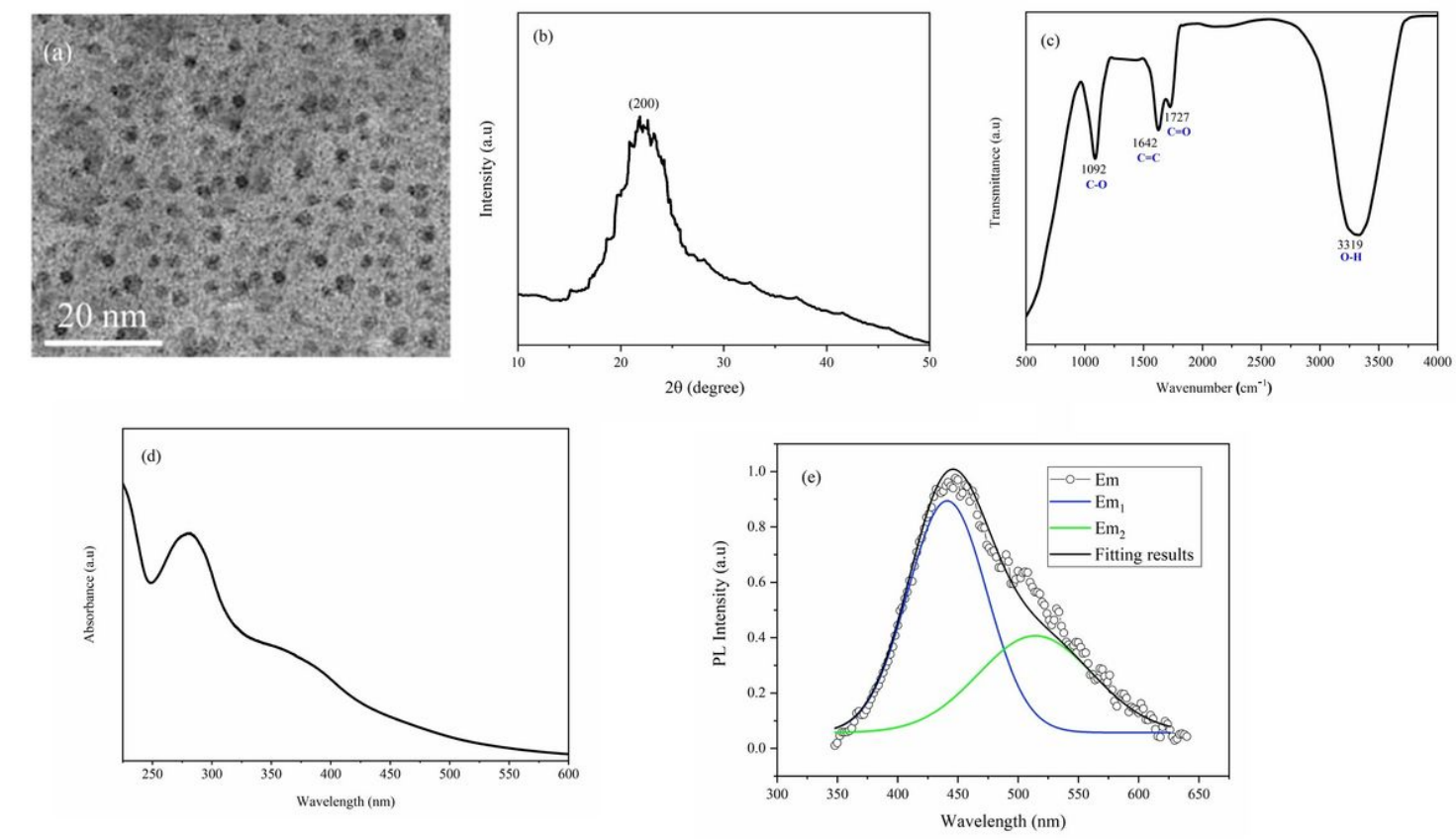

Figure 2

Characterization of CDs: (a) TEM images of CDs, (b) XRD pattern, (c) FTIR spectra of CDs, (d) UV-visible spectra, (e) PL spectra of CDs excited at 360 nm

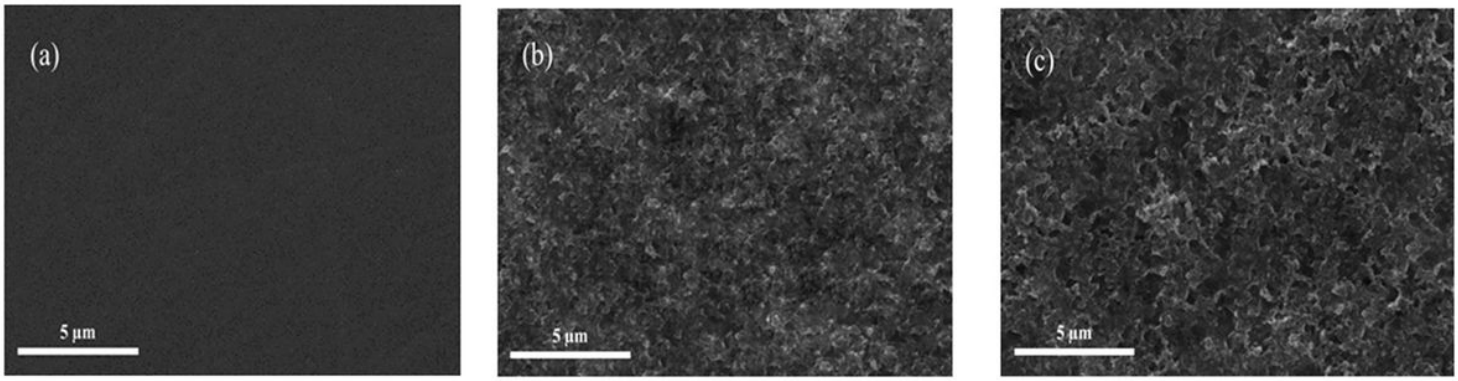

Figure 3

Images SEM of (a) bare GCE electrode, (b) CHITO/ GCE electrode, and (c) CHITO-CDs nanocomposite /GCE electrode

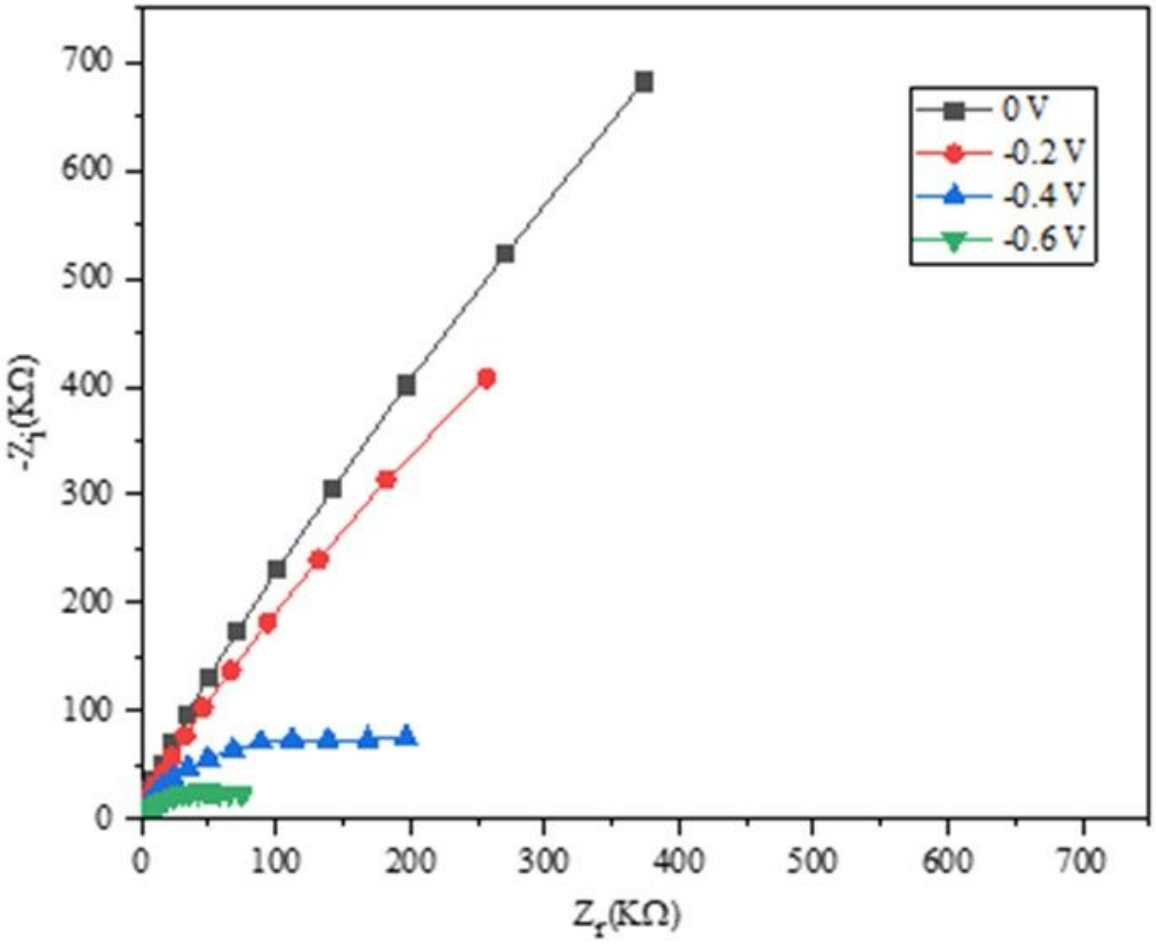

Figure 4

Impedance spectra of CHITO-CDs/GCE structure at different potentials (0, -0.2 V, -0.4 V, -0.6 V)

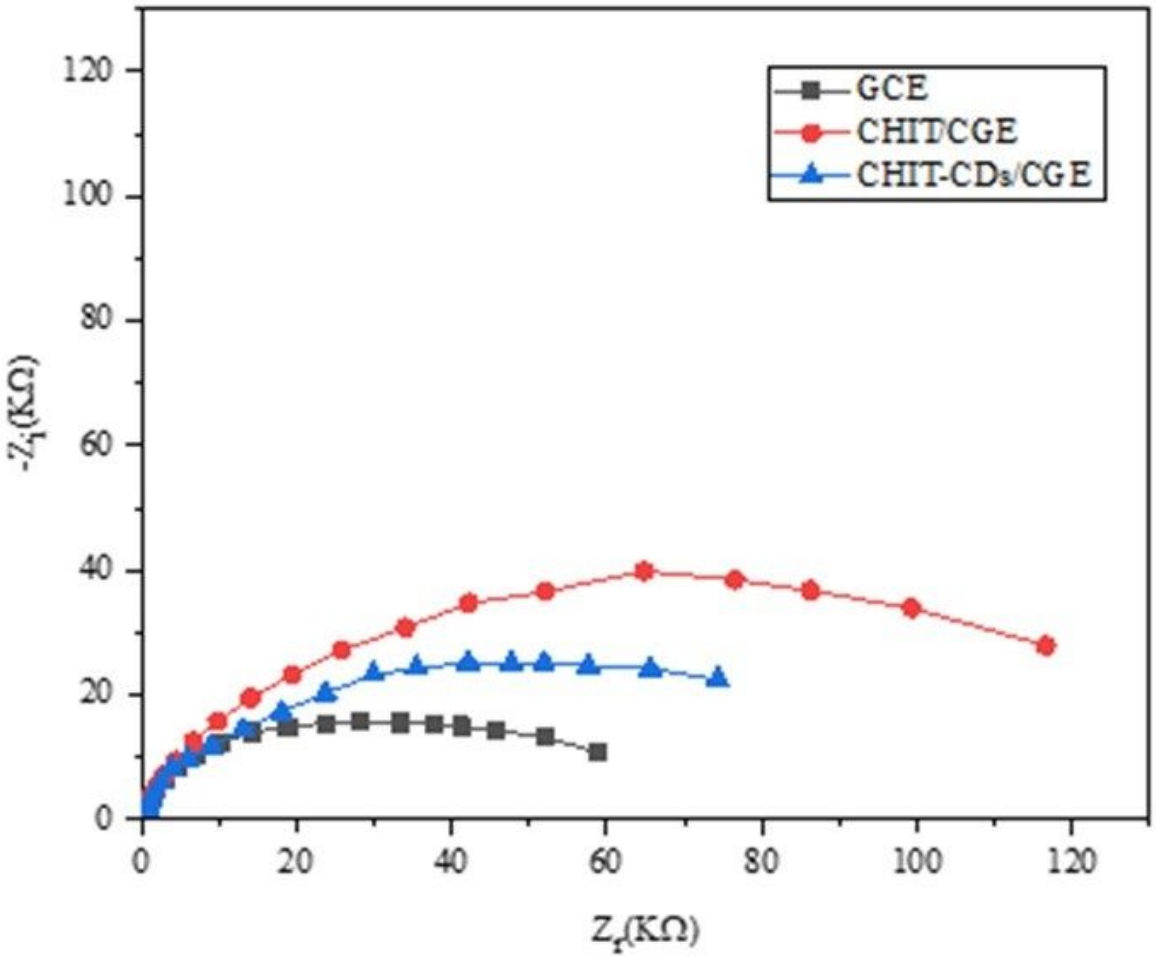

Figure 5

Impedance spectra of bare GCE, CHITO/GCE and CHITO-CDs /GCE structures

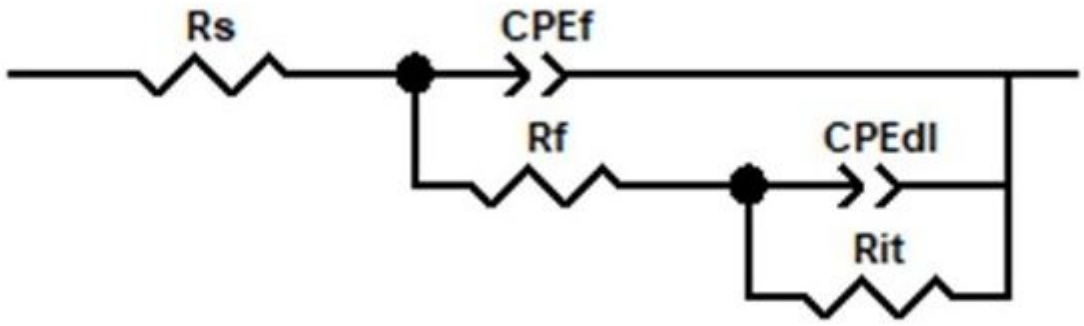

Figure 6

Equivalent circuit used to fit the impedance spectra

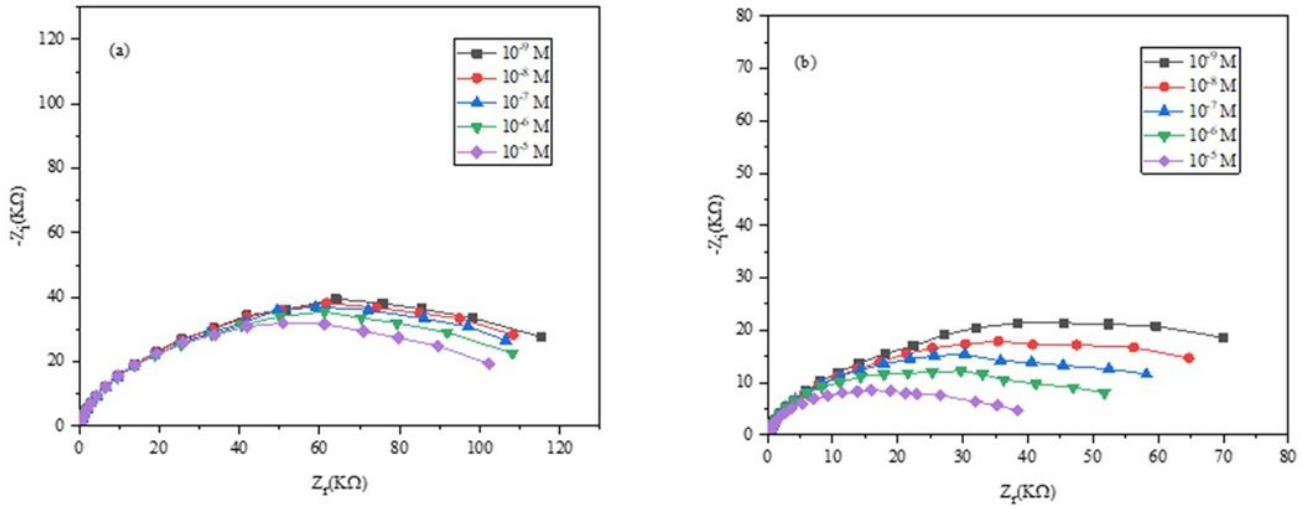

Figure 7

Impedance spectra for different copper concentrations of (a) CHITO/GCE and (b) CHITO-CDs/GCE

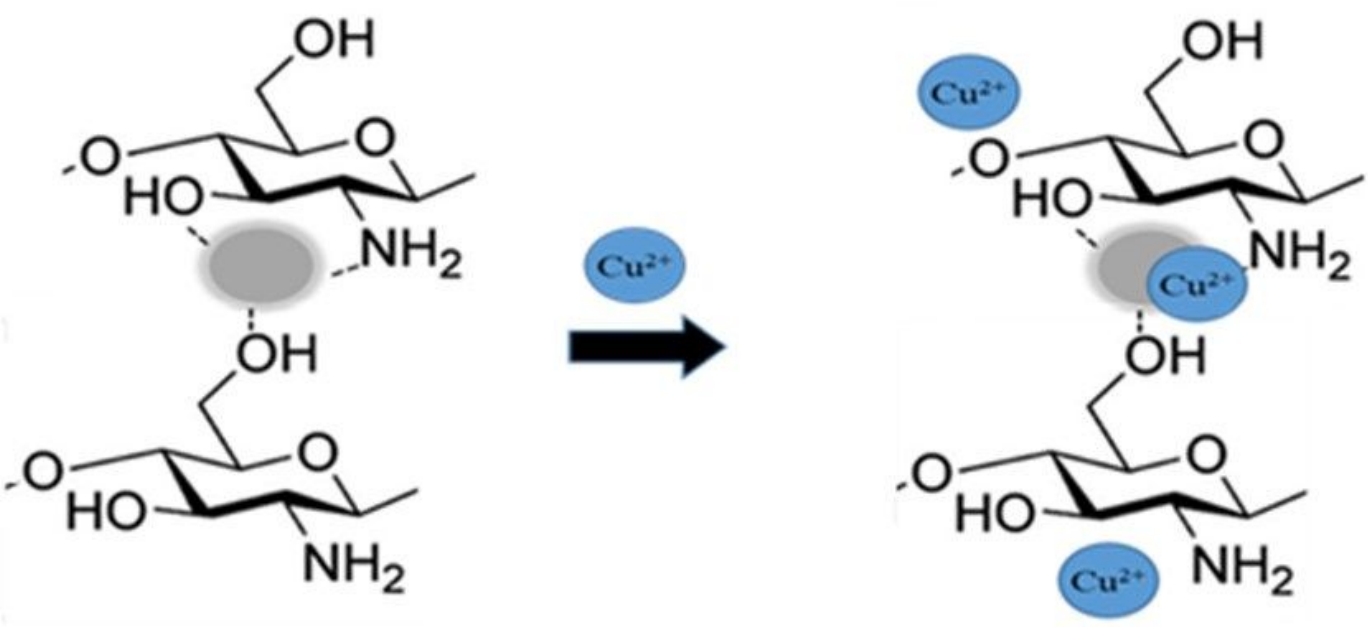

Figure 8

Schematic representation of detection toward copper ions by CHITO-CDs nanocomposite film

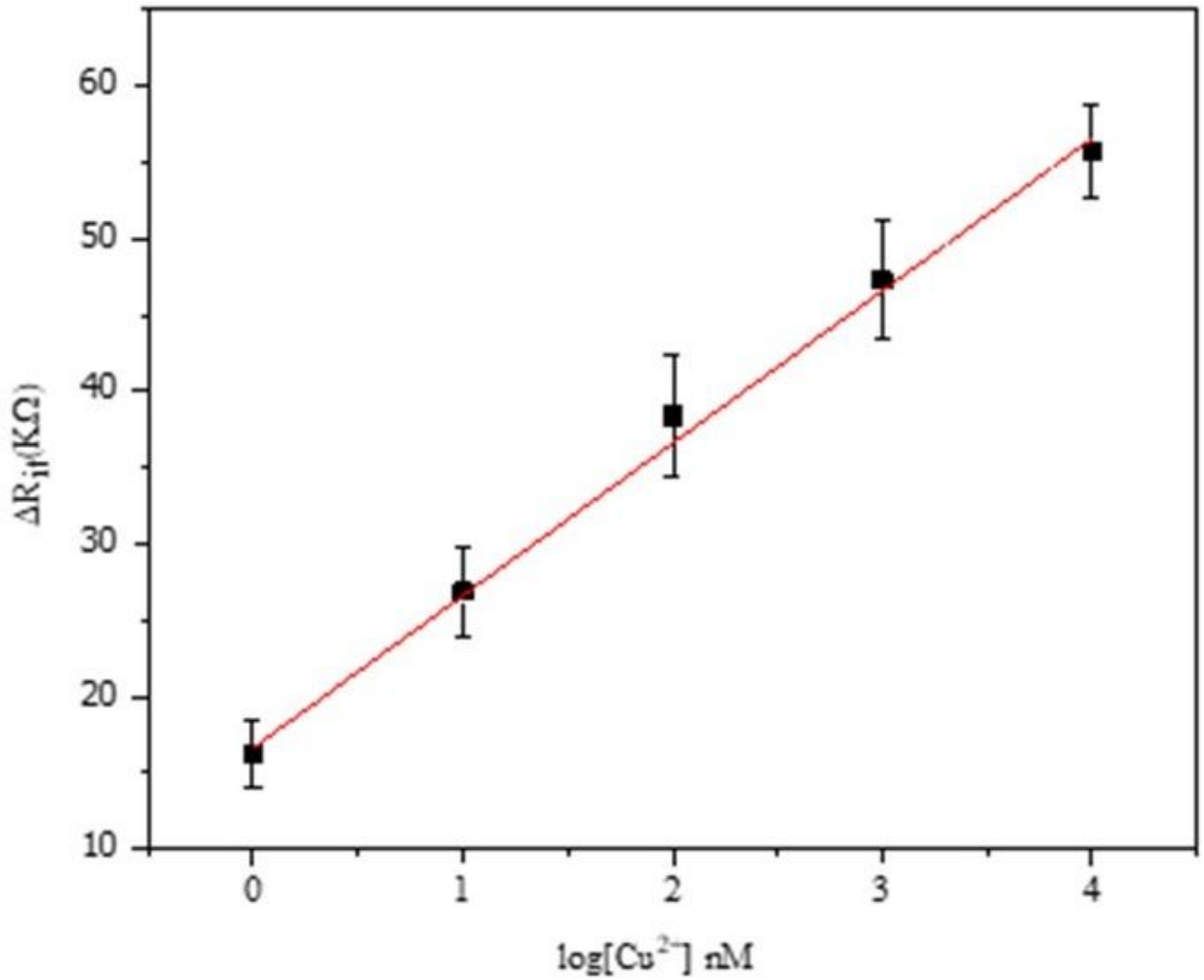

Figure 9

Calibration curve of ΔRit versus log ([Cu2+]/n□)

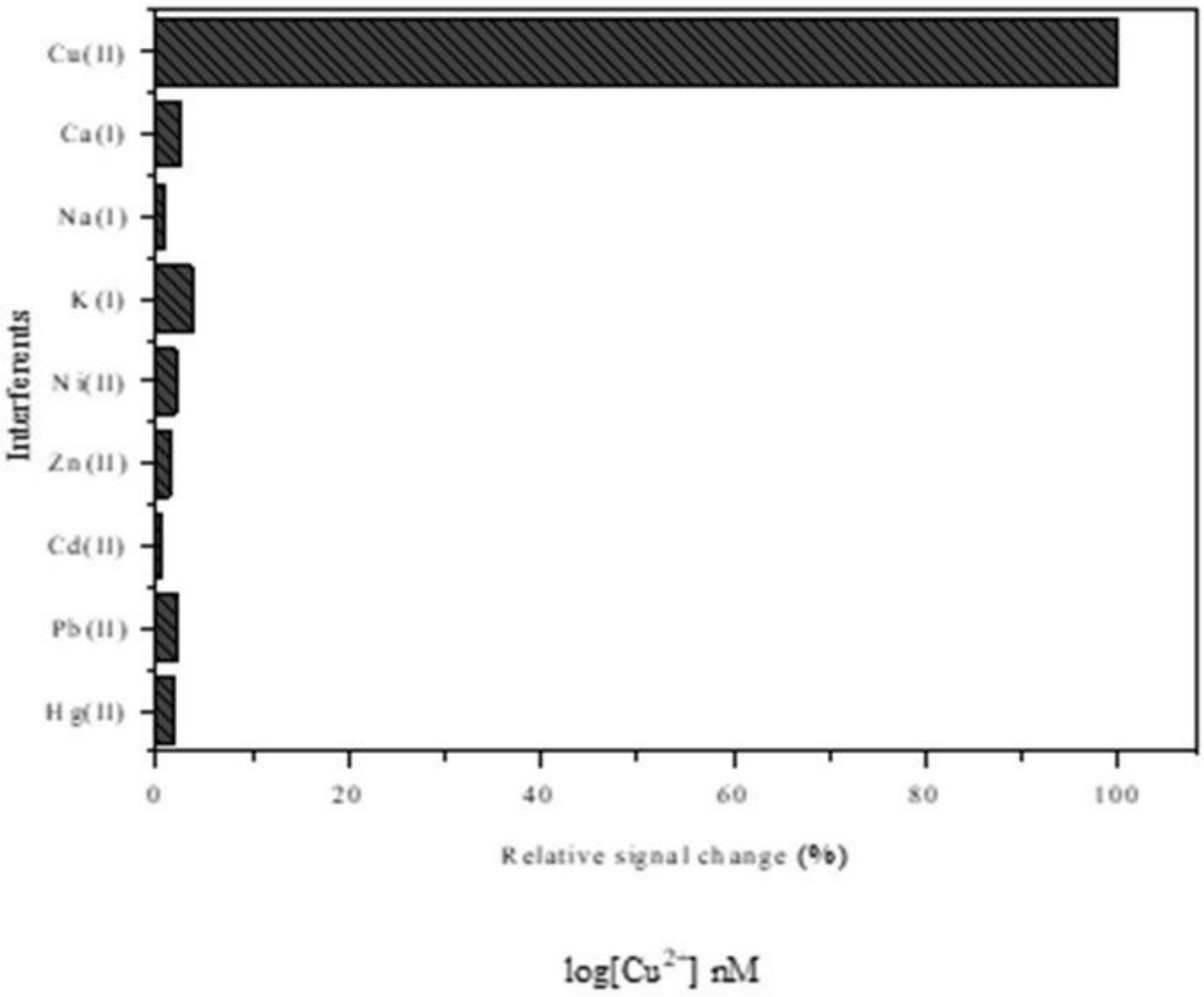

Figure 10

Influence of interferences (10-4 M) on the response Cu(II) ion (10-6 M)